JOC The Journal of Organic Chemistry

Article

pubs.acs.org/joc

Decarboxylative-Coupling of Allyl Acetate Catalyzed by Group 10 Organometallics, $[(phen)M(CH_3)]^+$

Matthew Woolley,[†,‡,§] Alireza Ariafard,*[,∥,⊥] George N. Khairallah,[†,‡,§] Kim Hong-Yin Kwan,[†,‡] Paul S. Donnelly,[†,‡] Jonathan M. White,[†,‡] Allan J. Canty,[∥] Brian F. Yates,[∥] and Richard A. J. O'Hair*[,†,‡,§]

[†]School of Chemistry, [‡]Bio21 Institute of Molecular Science and Biotechnology, and [§]ARC Centre of Excellence for Free Radical Chemistry and Biotechnology, The University of Melbourne, Melbourne, Victoria 3010, Australia

[∥]School of Physical Sciences, University of Tasmania, Private Bag 75, Hobart, Tasmania 7001, Australia

[⊥]Department of Chemistry, Faculty of Science, Central Tehran Branch, Islamic Azad University, Shahrak Gharb, Tehran 1467686831, Iran

Supporting Information

ABSTRACT: Gas-phase carbon−carbon bond forming reactions, catalyzed by group 10 metal acetate cations $[(phen)M(O_2CCH_3)]^+$ (where M = Ni, Pd or Pt) formed via electrospray ionization of metal acetate complexes $[(phen)M(O_2CCH_3)_2]$, were examined using an ion trap mass spectrometer and density functional theory (DFT) calculations. In step 1 of the catalytic cycle, collision induced dissociation (CID) of $[(phen)M(O_2CCH_3)]^+$ yields the organometallic complex, $[(phen)M(CH_3)]^+$, via decarboxylation. $[(phen)M(CH_3)]^+$ reacts with allyl acetate via three competing reactions, with reactivity orders (% reaction efficiencies) established via kinetic modeling. In step 2a, allylic alkylation occurs to give 1-butene and reform metal acetate, $[(phen)M(O_2CCH_3)]^+$, with Ni (36%) > Pd (28%) > Pt (2%). Adduct formation, $[(phen)M(C_6H_{11}O_2)]^+$, occurs with Pt (24%) > Pd (21%) > Ni(11%). The major losses upon CID on the adduct, $[(phen)M(C_6H_{11}O_2)]^+$, are 1-butene for M = Ni and Pd and methane for Pt. Loss of methane only occurs for Pt (10%) to give $[(phen)Pt(C_5H_7O_2)]^+$. The sequences of steps 1 and 2a close a catalytic cycle for decarboxylative carbon−carbon bond coupling. DFT calculations suggest that carbon−carbon bond formation occurs via alkene insertion as the initial step for all three metals, without involving higher oxidation states for the metal centers.

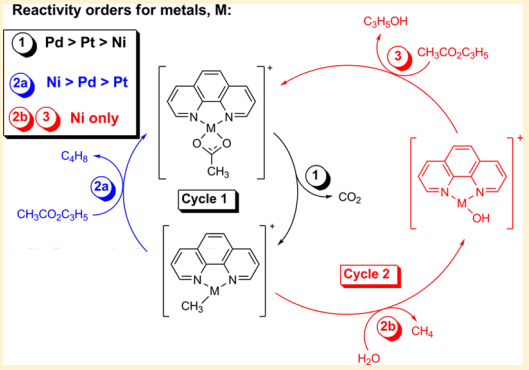

INTRODUCTION

The synthesis of complex organic molecules from simpler ones involves structural transformations that have been classified into three main groups of reactions: (i) carbon−carbon bond formation, (ii) oxidation/reduction, and (iii) functional group transformations.[1,2] The use of stoichiometric metal containing reagents and metal catalysts can play key roles in each of these classes of reactions.[3] Within the context of the 12 principles of "green chemistry",[4] the hunt continues for the ideal metal catalyzed reactions that result in C−X bond formation with excellent atom economy. Thermally induced metal catalyzed decarboxylation reactions have attracted significant recent interest because they exhibit excellent atom economy for the organic substrate, which only produces CO_2 as a byproduct, involve the use of widely available carboxylic acids[5] and their derivatives,[6] and are often more selective than thermolysis in the absence of a metal catalyst. With regards to the latter point, Tunge has developed Pd catalyzed decarboxylative allylation reactions (eq 1),[7,8] which are more selective than the competing radical fragmentation pathways that occur under pyrolysis of allyl carboxylates (e.g., eqs 2−4 for allyl acetate).[9]

$$RCO_2CH_2CH{=}CH_2 \rightarrow RCH_2CH{=}CH_2 + CO_2 \quad (1)$$

$$CH_3CO_2CH_2CH{=}CH_2 \rightarrow CH_3^{\bullet} + {}^{\bullet}CH_2CH{=}CH_2 + CO_2 \quad (2)$$

$$CH_3^{\bullet} + CH_3CO_2CH_2CH{=}CH_2 \rightarrow CH_3CH_2CH{=}CH_2 + CH_3^{\bullet} + CO_2 \quad (3)$$

$$\rightarrow CH_2{=}CHCHO + CH_4 + CH_3^{\bullet} + CO \quad (4)$$

Stoichiometric metal decarboxylation reactions involving the formation of organometallic intermediates date back to the pioneering work of Pesci, who reported in 1901 the isolation of the organomercury derivative formed from decomposition of phthalic acid (Scheme 1A).[10,11] In the 1920s, Whitmore showed that these organomercury derivatives could be transformed via reaction with HCl and Br_2 (Scheme 1A),[12] while Kharasch recognized the potential of using mercury mediated decarboxylation reactions in the construction of C−C bonds.[13] Thus, thermolysis of isolated organomercury com-

Special Issue: Mechanisms in Metal-Based Organic Chemistry

Received: August 15, 2014
Published: October 20, 2014

   dx.doi.org/10.1021/jo501886w | J. Org. Chem. 2014, 79, 12056−12069

Scheme 1. Examples of Stoichiometric and Catalyzed Metal Decarboxylation Reactions Involving the Intermediacy of Organometallic Species

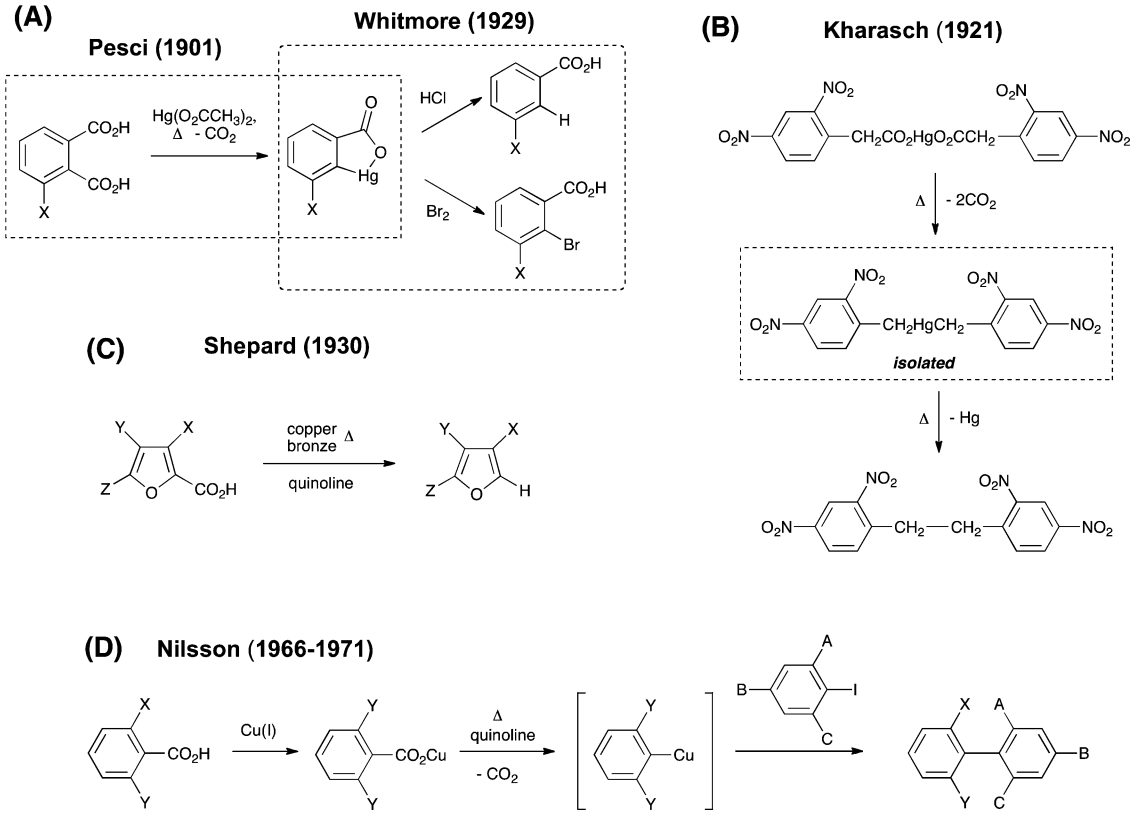

Scheme 2. Pd Catalyzed Allylation Alkylation Reactions: (A) Pd(II) Catalyzed Allyl-Aryl Coupling between Allylic Esters and Aryl Boronic Esters[18] (L = phen); (B) Pd(0) Catalyzed Decarboxylative Allylation Reactions (eq 1) Involving Decarboxylation of the Free Carboxylate Anion (L = Ph_3P)[20]

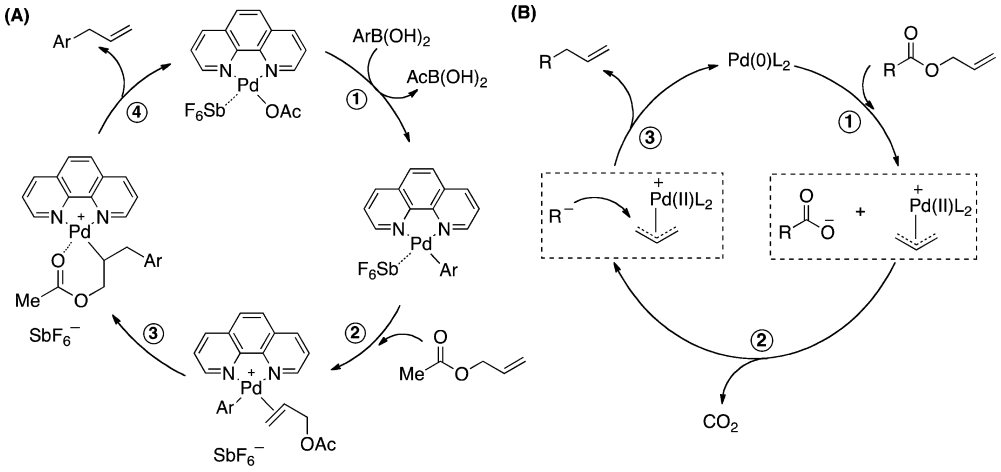

pounds formed from decarboxylation proceeds via reductive elimination to yield the C−C coupled product and metallic mercury (Scheme 1B). The first examples of metal catalyzed decarboxylative transformations of carboxylic acids include the copper catalyzed protodecarboxylation of furans (Scheme 1C)[14] and decarboxylative coupling reactions reported by Nilsson (Scheme 1D).[15] More recently, the discovery of palladium catalyzed decarboxylative coupling reactions of aryl carboxylic acids by Myers[16] and Goossen[17] have spurred numerous studies of metal catalyzed decarboxylative coupling reactions.[5]

Transition metal catalyzed allylic alkylation reactions have become important carbon−carbon bond forming methods in organic synthesis, and there is continued interest in developing new variants that offer regioselective and enantioselective control as a result of the operation of different mechanisms.[18] Allyl carboxylates have been widely used as substrates in allylic alkylation reactions, although the R group of resultant carboxylate is often "wasted". For example, Sawamura has developed Pd(II) catalyzed allyl−aryl coupling between allylic esters and aryl boronic esters.[18] Based upon isolation of Pd(II) complexes from stoichiometric reactions, a mechanism was

dx.doi.org/10.1021/jo501886w | J. Org. Chem. 2014, 79, 12056−12069

proposed (Scheme 2A) in which C−C bond formation involves coordination of allyl acetate as a conventional η^2-alkene (step 2) followed by insertion (step 3) and then β-OAc elimination (step 4).[18a,b,d] In contrast, Tunge[6,7] and Chruma[19] have developed Pd(0) catalyzed decarboxylative allylation reactions in which the R group of carboxylate is used (eq 1). Recent theoretical work suggests a mechanism involving insertion into the O−C bond to form a π-allyl Pd cation and a free carboxylate anion (step 1, Scheme 2B), with the free carboxylate anion undergoing decarboxylation (step 2) followed by an outer sphere C−C bond coupling reaction (step 3).[20,21]

We have been using the powerful combination of multistage mass spectrometry (MS^n) experiments in ion trap mass spectrometers[22] and DFT calculations[23] to examine the formation of organometallic ions via decarboxylation of metal carboxylate ions[24] and their subsequent unimolecular[25] and bimolecular reactions.[26] Unimolecular reactions have been discovered that result in C−C bond formation including dehydrodecarboxylative coupling of acetate ligands (eq 5) by the sequential reactions shown in eq 6[25b] and Glaser like decarboxylative coupling of two alkynoate ligands (eq 7)[25c] by the sequential reactions shown in eq 8.

$$2CH_3CO_2^- \rightarrow CH_2{=}CH_2 + 2CO_2 + 2H^- \quad (5)$$

$$[Cu(O_2CCH_3)_2]^- \xrightarrow[MS^2]{-CO_2} [CH_3Cu(O_2CCH_3)]^- \xrightarrow[MS^3]{-CO_2} [Cu(CH_3)_2]^- \xrightarrow[MS^4]{-CH_2=CH_2} [CuH_2]^- \quad (6)$$

$$2RC{\equiv}CCO_2^- \rightarrow (RC{\equiv}C)_2 + 2CO_2 + 2e^- \quad (7)$$

$$[Co_nCl_{2n-1}(O_2CR)_2]^- \xrightarrow[MS^2]{-CO_2} [Co_nCl_{2n-1}(R)O_2CR)]^- \xrightarrow[MS^3]{-CO_2} [Co_nCl_{2n-1}(R)_2]^- \xrightarrow[MS^4]{-R_2} [Co_nCl_{2n-1}]^- \quad (8)$$

Stoichiometric C−C bond coupling reactions of coinage metal organometallic ions with methyl iodide[26a,b] and allyl iodide[26c,d] have been reported, and by changing the leaving group from iodide, we uncovered catalytic cycles (Scheme 3)

Scheme 3. Copper Catalyzed Decarboxylative Allylation of Allyl Acetate (eq 1) Involving Formation of the Organocopper Intermediate[26e,f]

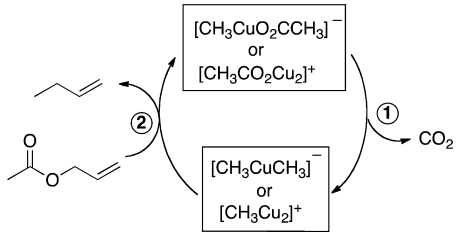

for the decarboxylative coupling of allyl acetate (eq 1, R = CH_3) utilizing dimethyl cuprate, $[CH_3CuCH_3]^-$, or the cluster $[CH_3Cu_2]^+$ as the catalyst.[26e,f,27] Unlike the decarboxylative allylation reactions developed by Tunge[6,7] and Chruma,[19] these copper catalyzed reactions (Scheme 3) involve the formation of an organometallic species via decarboxylation (step 1 of Scheme 3) followed by subsequent C−C bond coupling (step 2).

We have recently described a catalytic cycle for the gas phase protodecarboxylation of acetic acid (eq 9 and Scheme 4, where

Scheme 4. Competing Catalytic Cycles for Protodecarboxylation, R = H (eq 9), and Decarboxylative Allylation of Allyl Acetate, R = $CH_2CH{=}CH_2$ (eq 1, R = CH_3)[a]

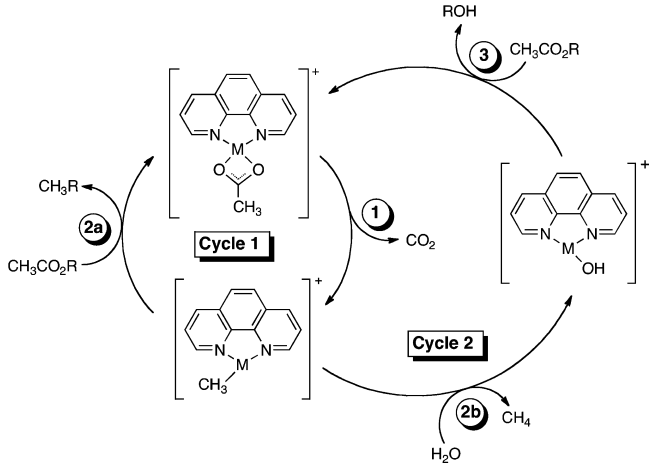

[a]In the case of acetic acid, the outcome of cycles 1 and 2 is equivalent (eq 9). In the case of allyl acetate, cycle 2 is a competing catalytic cycle for the water catalyzed decomposition of allyl acetate (eq 15).

R = H) that is catalyzed by group 10 organometallics, $[(phen)M(CH_3)]^+$,[28] which are formed by decarboxylation (eq 10) in competition with loss of an acetate radical (eq 11).[29] In the case of Ni, a competing water mediated catalytic cycle was discovered (cycle 2, Scheme 4), which involves an initial hydrolysis reaction (eq 12) followed by reaction with acetic acid (eq 13).

$$CH_3CO_2H \rightarrow CH_4 + CO_2 \quad (9)$$

$$[(phen)M(O_2CCH_3)]^+ \rightarrow [(phen)M(CH_3)]^+ + CO_2 \quad (10)$$

$$\rightarrow [(phen)M]^{+\cdot} + CH_3CO_2^{\cdot} \quad (11)$$

$$[(phen)M(CH_3)]^+ + H_2O \rightarrow [(phen)M(OH)]^+ + CH_4 \quad (12)$$

$$[(phen)Ni(OH)]^+ + CH_3CO_2H \rightarrow [(phen)Ni(O_2CCH_3)]^+ + H_2O \quad (13)$$

Here we describe a catalytic cycle for the gas phase decarboxylative allylation of allyl acetate (eq 1, R = CH_3) catalyzed by the same group 10 organometallics. The first step of both catalytic cycles is decarboxylation (eq 10 and step 1 of Scheme 4), so here we focus on the allylation reactions of $[(phen)M(CH_3)]^+$ with allyl acetate (eq 14). Of particular interest is whether these coupling reactions proceed via mechanisms involving the formation of metal(IV) intermediate[30] by oxidative addition followed by reductive elimination[31] or via an isohypsic mechanism[32] within a Pd(II) manifold related to that proposed by Sawamura (steps 2−4 of Scheme 2a)[18] and whether $[(phen)Ni(CH_3)]^+$ undergoes a competing catalytic cycle for the water catalyzed decomposition of allyl acetate (eq 15, cycle 2 of Scheme 4, R′ = $CH_2CH{=}CH_2$) proceeding via hydrolysis (eq 12) followed by reaction with allyl actetate (eq 16).

dx.doi.org/10.1021/jo501886w | J. Org. Chem. 2014, 79, 12056−12069

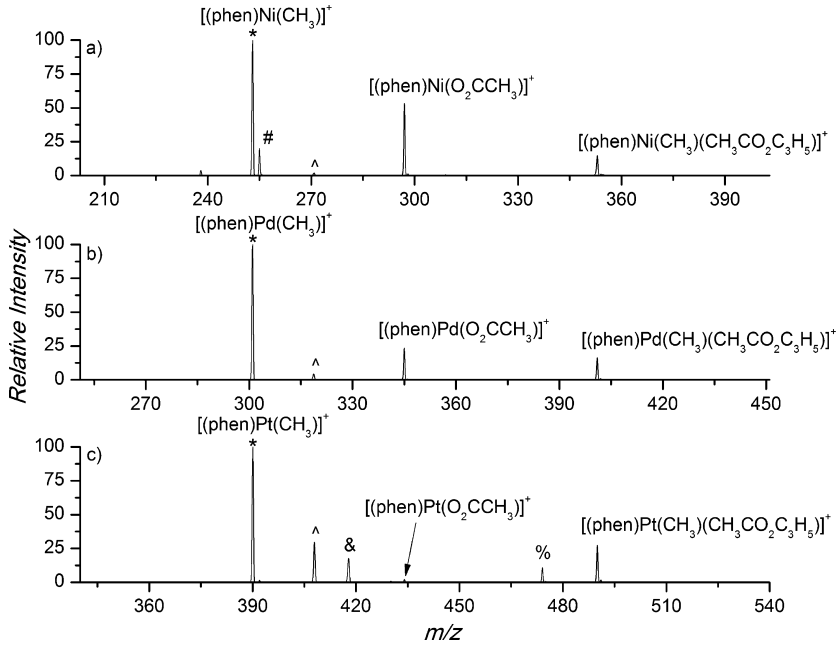

Figure 1. LTQ-FT-ICR MS^3 spectra of ion−molecule reactions of mass selected organometallic ions with allyl acetate (~5×10^9 molecules/cm^3) for a period of 100 ms in the linear ion trap: (a) $[(phen)^{58}Ni(CH_3)]^+$; (b) $[(phen)^{106}Pd(CH_3)]^+$; (c) $[(phen)^{195}Pt(CH_3)]^+$. The mass selected organometallic ions are denoted by ∗, # represents the product of hydrolysis for $[(phen)M(CH_3)]^+$, ∧ represents the product formed via addition of water to $[(phen)M(CH_3)]^+$, & represents the product formed via addition of N_2 to $[(phen)M(CH_3)]^+$. % represents the product $[(phen)Pt(C_5H_7O_2)]^+$ formed via loss of methane from the adduct.

$$[(phen)M(CH_3)]^+ + CH_3CO_2CH_2CH{=}CH_2 \rightarrow [(phen)M(O_2CCH_3)]^+ + CH_3CH_2CH{=}CH_2 \quad (14)$$

$$CH_3CO_2CH_2CH{=}CH_2 + H_2O \rightarrow HOCH_2CH{=}CH_2 + CO_2 + CH_4 \quad (15)$$

$$[(phen)M(OH)]^+ + CH_3CO_2CH_2CH{=}CH_2 \rightarrow [(phen)M(O_2CCH_3)]^+ + HOCH_2CH{=}CH_2 \quad (16)$$

RESULTS AND DISCUSSION

The organometallic complexes $[(phen)M(CH_3)]^+$ were generated in the gas phase in a series of MS^2 experiments via decarboxylation of the acetate complexes $[(phen)M(O_2CCH_3)]^+$ under conditions of collision-induced dissociation (CID). This process has been described in detail previously,[28] so the focus herein is on establishing whether $[(phen)M(CH_3)]^+$ reacts with allyl acetate via allylation (eq 14 and step 2a of Scheme 4).

Gas Phase Ion−Molecule Reactions of $[(phen)M(CH_3)]^+$ with Allyl Acetate. The organometallic cations $[(phen)M(CH_3)]^+$, **4**, were mass selected in a series of MS^3 experiments and allowed to undergo ion−molecule reactions with allyl acetate introduced into the LTQ mass spectrometer (Figure 1). Product ion assignments were confirmed by high-resolution mass spectrometry experiments (Supporting Information, Table S1), as well as by using the deuterium labeled analogue $[(phen)M(CD_3)]^+$ (Supporting Information, Figure S1).[33] Each of the organometallic ions $[(phen)M(CH_3)]^+$ reacted with allyl acetate to regenerate the carboxylate, (eq 14) completing a catalytic cycle for the decarboxylative formation of 1-butene via carbon−carbon bond formation (eq 1, where R = CH_3).

The major product formed via reaction between $[(phen)Ni(CH_3)]^+$ (m/z 253, Figure 1a) and allyl acetate is $[(phen)Ni(O_2CCH_3)]^+$ (m/z 297, eq 14). Formation of the adduct $[(phen)Ni(C_6H_{11}O_2)]^+$ (m/z 353, eq 17) is also observed, and the structure of this adduct was interrogated via CID as discussed below. The hydrolysis product $[(phen)Ni(OH)]^+$ (m/z 255, eq 12) and the water adduct $[(phen)Ni(CH_3)(H_2O)]^+$ (m/z 271, eq 18) are both minor products that arise from the presence of adventitious water and have been previously examined in detail.[34]

$$[(phen)M(CH_3)]^+ + CH_3CO_2CH_2CH{=}CH_2 \rightarrow [(phen)M(C_6H_{11}O_2)]^+ \quad (17)$$

$$[(phen)M(CH_3)]^+ + H_2O \rightarrow [(phen)M(CH_3)(H_2O)]^+ \quad (18)$$

The main products in the reaction of $[(phen)Pd(CH_3)]^+$ with allyl acetate (m/z 301, Figure 1b) are the carboxylate, $[(phen)Pd(O_2CCH_3)]^+$ (m/z 345, eq 14), as well as the adduct $[(phen)Pd(C_6H_{11}O_2)]^+$ (m/z 401, eq 17). A minor product arising from addition of water to form $[(phen)Pd(CH_3)(H_2O)]^+$ (m/z 319, eq 18) is also detected.[34]

The reaction of $[(phen)Pt(CH_3)]^+$ (m/z 390, Figure 1c) with allyl acetate gives a richer spectrum. In contrast to the nickel and palladium cases, the carboxylate ion, $[(phen)Pt(O_2CCH_3)]^+$ (m/z 434, eq 14), is a minor product. The most abundant products arise from addition of allyl acetate to generate $[(phen)Pt(C_6H_{11}O_2)]^+$ (m/z 490, eq 17) and loss of methane from the adduct to give the ion $[(phen)Pt(C_5H_7O_2)]^+$ (m/z 474, eq 19), a reaction that is unique to platinum. There are two possible structures for this ion which depend on the site of H loss from allylacetate: the metal enolate complex,

dx.doi.org/10.1021/jo501886w | J. Org. Chem. 2014, 79, 12056−12069

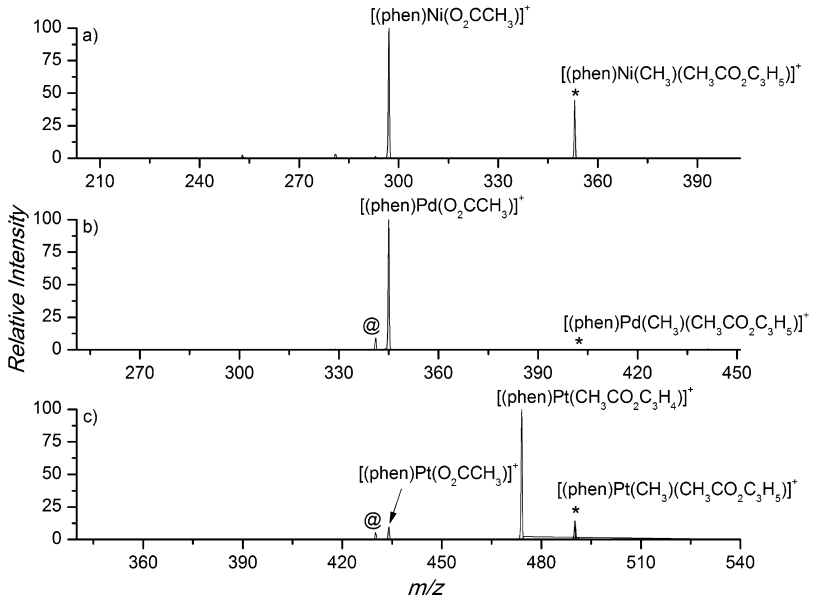

Figure 2. LTQ-FT-ICR MS^4 spectra of mass selected ions undergoing CID at a normalized collision energy of 25 (arbitrary units) in the linear ion trap: (a) $[(phen)^{58}Ni(CH_3)(CH_3CO_2C_3H_5)]^+$; (b) $[(phen)^{106}Pd(CH_3)(CH_3CO_2C_3H_5)]^+$; (c) $[(phen)^{195}Pt(CH_3)(CH_3CO_2C_3H_5)]^+$. The mass selected precursor ions are denoted by ∗, @ represents the product arising from loss of acetic acid (eq 22).

$[(phen)Pt(CH_2CO_2CH_2CHCH_2)]^+$,[35] or the allyl complex, $[(phen)Pt(CH_2CHCHO_2CCH_3)]^+$.[36] Reactions with adventitious neutrals, which have been previously described,[34a] include addition of water, $[(phen)Pt(CH_3)(H_2O)]^+$ (m/z 408, eq 18), hydrolysis, $[(phen)Pt(OH)]^+$ (m/z 392, eq 12), and addition of N_2 to yield $[(phen)Pt(CH_3)(N_2)]^+$ (m/z 418, eq 20).

$$[(phen)M(CH_3)]^+ + CH_3CO_2CH_2CH{=}CH_2 \rightarrow [(phen)M(C_5H_7O_2)]^+ + CH_4 \quad (19)$$

$$[(phen)M(CH_3)]^+ + N_2 \rightarrow [(phen)M(CH_3)(N_2)]^+ \quad (20)$$

Isotope labeling was used to establish the reaction channels. Reaction of $[(phen)M(CD_3)]^+$ with allyl acetate (Supporting Information, Figures S1) and of $[(phen)M(CH_3)]^+$ and $[(phen)M(CD_3)]^+$ with the two deuterium labeled allyl acetates, $CD_3CO_2CH_2CH{=}CH_2$ (Supporting Information, Figures S2 and S3) and $CH_3CO_2CD_2CH{=}CH_2$ (Supporting Information, Figures S4 and S5) allowed us to (i) confirm that the acetate in the product complex, $[(phen)M(O_2CCH_3)]^+$, comes from the allyl acetate, (ii) establish that methane loss (eq 19) can operate by both mechanisms, with deuterium isotope effects favoring the formation of the allyl complex, $[(phen)Pt(CH_2CHCHO_2CCD_3)]^+$ (m/z 477), in the case $CD_3CO_2CH_2CH{=}CH_2$ (Supporting Information, Figures S2 and S3) and the metal enolate complex, $[(phen)Pt(CH_2CO_2CD_2CHCH_2)]^+$ (m/z 476), in the case $CH_3CO_2CD_2CH{=}CH_2$ (Supporting Information, Figures S4 and S5).

CID of the Adducts. The fact that adduct formation (eq 17) is observed in all cases raises an interesting question: what are the structures of these adducts?[37] A number of scenarios are possible, including that they are (i) reactant association complexes formed between the organometallic ion and allyl acetate, $[(phen)M(CH_3)(CH_3CO_2C_3H_5)]^+$, that have failed to go on to C−C bond formation, (ii) intermediates (cf. complexes formed from steps 2 and 3 of Scheme 2A) along the C−C bond formation pathway that have been trapped via collisional cooling by the helium bath gas, or (iii) product association complexes between the metal acetate complexes and 1-butene, $[(phen)M(O_2CCH_3)(C_4H_8)]^+$. In order to further interrogate the structures of these $[(phen)M(C_6H_{11}O_2)]^+$ complexes, they were mass-selected and subjected to CID in a series of MS^4 experiments (Figure 2).[38] The dominant product for the Ni and Pd complexes arises from loss of 1-butene (eq 21). In addition for Pd, a minor channel arises from loss of acetic acid (eq 22). The observation of these two product channels suggest that they arise from a common intermediate, which corresponds to the product association complex, $[(phen)M(O_2CCH_3)(C_4H_8)]^+$, or an intermediate along the pathway to C−C bond coupling. In the case of Pt, loss of 1-butene (eq 21) and acetic acid (eq 22) are minor, while loss of methane (eq 23) is the major reaction channel. This suggests that the Pt complex is a mixture of the reactant association complex, $[(phen)Pt(CH_3)(CH_3CO_2C_3H_5)]^+$, and the product association complex, $[(phen)Pt(O_2CCH_3)(C_4H_8)]^+$.

$$[(phen)M(O_2CCH_3)(C_4H_8)]^+ \rightarrow [(phen)M(O_2CCH_3)]^+ + CH_3CH_2CH{=}CH_2 \quad (21)$$

$$\rightarrow [(phen)M(C_4H_7)]^+ + CH_3CO_2H \quad (22)$$

$$[(phen)M(CH_3)(CH_3CO_2C_3H_5)]^+ \rightarrow [(phen)M(CH_3CO_2C_3H_4)]^+ + CH_4 \quad (23)$$

Formation of "Off Cycle" Byproducts: Reactions of $[(phen)Ni(OH)]^+$and $[(phen)M]^{+\bullet}$ (M = Ni and Pd) with Allyl Acetate. A competing product in the first stage of CID is the radical cation, $[(phen)M]^{+\bullet}$ (M = Ni and Pd), which is formed via bond homolysis (eq 11). In addition, the organometallic ions $[(phen)M(CH_3)]^+$, **4**, can react with background water to form the hydroxide (eq 12), a reaction that can close a competing second cycle (cycle 2 of Scheme 4), especially in the case of Ni. Thus, it was of interest to examine the reactions of mass selected $[(phen)M]^{+\bullet}$ (M = Ni and Pd)

dx.doi.org/10.1021/jo501886w | J. Org. Chem. 2014, 79, 12056−12069

Scheme 5. Kinetic Model for the Competing Reactions of $[(phen)M(CH_3)]^+$ Used To Extract Kinetic Data for the Formation of the Collisionally Stabilized Adduct, $[(phen)M(CH_3)(C_3H_5O_2CC_3H_5)]^+$, the Product Arising from CH_4 Loss, $[(phen)M(C_5H_7O_2)]^+$, and the Carbon−Carbon Bond Formation Product, $[(phen)M(O_2CCH_3)]^+$[a]

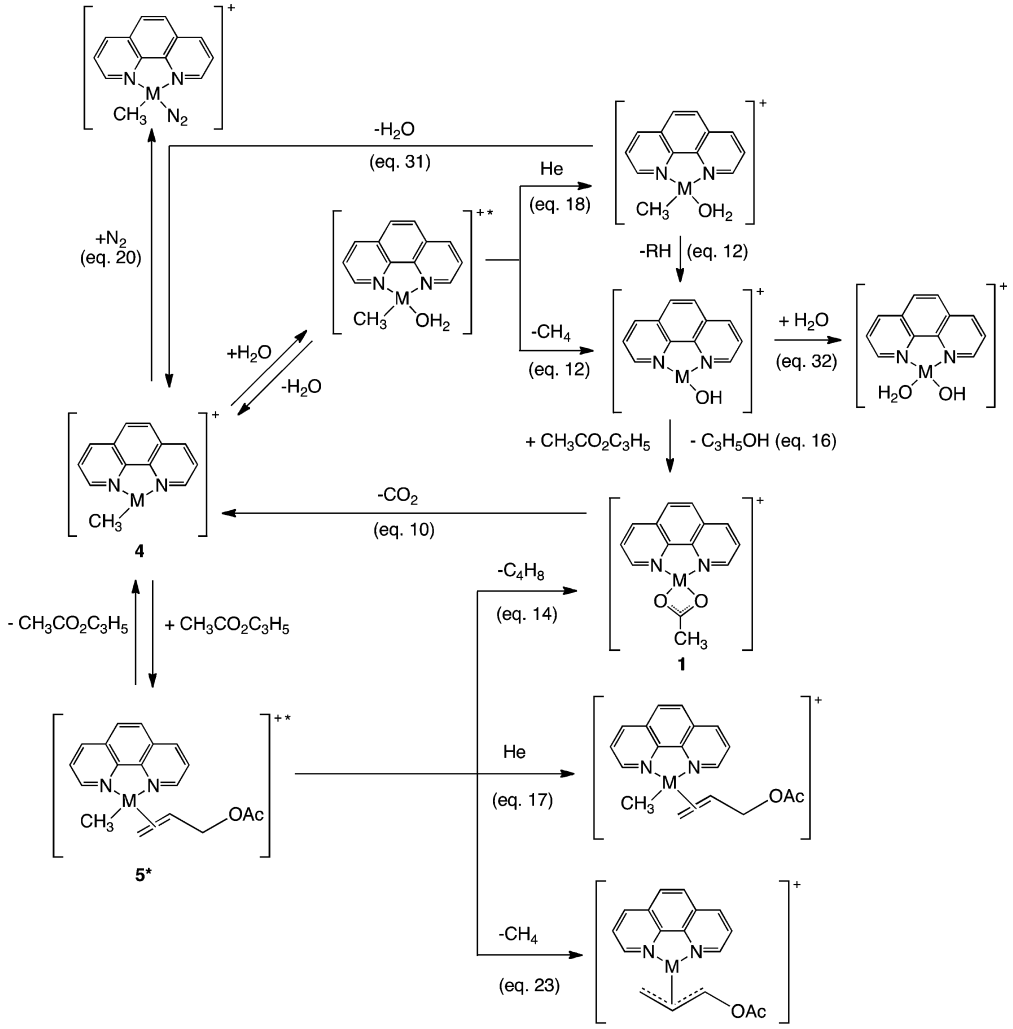

[a]Note that adduct formation (eq 17) was found to be irreversible.

and $[(phen)Ni(OH)]^+$ with allyl acetate since these could lead to the formation of "off cycle" byproducts.

The main product of the reaction of $[(phen)Ni(OH)]^+$ with allyl acetate is the adduct (eq 24), while only a trace amount of the acetate (eq 16) is formed (Supporting Information, Figure S6a). Mass selection of the adduct followed by CID mainly regenerates $[(phen)Ni(OH)]^+$ (Supporting Information, Figure S6b), which is indicative of the reactant association complex $[(phen)Ni(OH)(CH_3CO_2C_3H_5)]^+$ (eq 25), although a minor amount of the acetate is also observed, which likely arises from the product association complex, $[(phen)Ni(O_2CCH_3)(C_3H_5OH)]^+$ (eq 26). These results suggest that step 3 of cycle 2 is inefficient.

$$[(phen)Ni(OH)]^+ + CH_3CO_2CH_2CH{=}CH_2 \rightarrow [(phen)Ni(C_5H_9O_3)]^+ \quad (24)$$

$$[(phen)Ni(OH)(CH_3CO_2C_3H_5)]^+ \rightarrow [(phen)Ni(OH)]^+ + CH_3CO_2C_3H_5 \quad (25)$$

$$[(phen)Ni(O_2CCH_3)(C_3H_5OH)]^+ \rightarrow [(phen)Ni(O_2CCH_3)]^+ + C_3H_5OH \quad (26)$$

The radical cations $[(phen)M]^{+\bullet}$ (M = Ni and Pd) react with allyl acetate via adduct formation (eq 27) and to regenerate the acetate via loss of an allyl radical (eq 28; Supporting Information, Figure S7). CID of the adduct leads to allyl radical loss (eq 29), as well as regeneration of $[(phen)M]^{+\bullet}$ (eq 30; Supporting Information, Figure S8). Reactions 11 and 28 thus close a catalytic cycle for the metal catalyzed radical induced decomposition of allyl acetate, most likely related to that observed for pyrolysis (eq 2).[9,29]

$$[(phen)M]^{+\cdot} + CH_3CO_2C_3H_5 \rightarrow [(phen)M(CH_3CO_2C_3H_5)]^{+\cdot} \quad (27)$$

$$\rightarrow [(phen)M(O_2CCH_3)]^+ + C_3H_5^{\cdot} \quad (28)$$

$$[(phen)M(CH_3CO_2C_3H_5)]^{+\cdot} \rightarrow [(phen)M(O_2CCH_3)]^+ + C_3H_5^{\cdot} \quad (29)$$

$$\rightarrow [(phen)M]^{+\cdot} + CH_3CO_2C_3H_5 \quad (30)$$

dx.doi.org/10.1021/jo501886w | J. Org. Chem. 2014, 79, 12056−12069

Extraction of kinetic Data for the C−C Bond Coupling Reaction via Modeling of the Kinetics Associated with Competing Reaction Pathways. The reactivity orders of $[(phen)M(CH_3)]^+$ toward allyl acetate were established via kinetic measurements in which the $[(phen)M(CH_3)]^+$ ions were isolated within the ion trap for varying periods of time in the presence of a known concentration of allyl acetate. Due to the occurrence of multiple competing (i.e., eqs 12, 14, 17, 18, 19, and 20) and sequential reactions (e.g., eqs 12 and 16) within the ion trap, the extraction of rate constants for the primary reactions of $[(phen)M(CH_3)]^+$ with allyl acetate alone is nontrivial. To help establish which secondary reactions are important, additional MS^4 experiments were performed in which the primary product ions $[(phen)M(OH)]^+$, $[(phen)M(CH_3)(H_2O)]^+$, and $[(phen)M(CH_3)(N_2)]^+$ formed via eqs 12, 18, and 20 were mass selected and allowed to undergo further reaction. While $[(phen)Ni(OH)]^+$ reacts via adduct formation (eq 24) and C−O bond coupling (eq 16; Supporting Information, Figure S6), both four-coordinate complexes $[(phen)M(CH_3)(H_2O)]^+$ and $[(phen)M(CH_3)(N_2)]^+$ were unreactive (Supporting Information, Figure S9). This allowed us to formulate the reaction mechanism (Scheme 5) of all potentially significant pathways associated with the reaction of $[(phen)M(CH_3)]^+$ and allyl acetate and background gases in the ion trap mass spectrometer. A phenomenological kinetic model was then constructed featuring individual rate constants for each identified step, and the rate constant values were determined numerically by fitting experimentally measured concentration (ion abundances) vs time data for the ions $[(phen)M(CH_3)]^+$, $[(phen)M(O_2CCH_3)]^+$, $[(phen)M(CH_3)(H_2O)]^+$, $[(phen)M(OH)]^+$, $[(phen)M(CH_3)(N_2)]^+$, $[(phen)M(OH)(H_2O)]^+$, $[(phen)M(CH_3)(CH_3CO_2C_3H_5)]^+$, and $[(phen)M(CH_3CO_2C_3H_4)]^+$ based upon a least-squares regression. These calculations were performed using the DynaFit program[39] and are similar to other kinetic modeling efforts described previously.[38a] The results are summarized in Table 1 along with the reaction efficiencies determined by comparison of the experimental rate constants to the theoretical ADO rate constants as determined using the program Colrate.[40−42]

DFT Calculated Mechanisms for Reaction of$[(phen)M(CH_3)]^+$with Allyl Acetate. Potential mechanisms for carbon−carbon bond formation (eq 14) between $[(phen)M(CH_3)]^+$ and allyl acetate and formation of the enolate (eq 19) were explored using DFT calculations.[43]

Mechanisms for Carbon−Carbon Bond Formation. Two different general mechanisms were examined for carbon−carbon bond formation with initial interactions involving oxidation of the metal center[44] or alkene insertion[18] because these are observed protocols with other reagents in the organometallic chemistry of these metals. Six mechanisms for oxidation were explored, summarized in Figure 3 showing three precursor species (**2_M**, **5_M**, **7_M**) and the transition structures arising from them. The lowest energy process is shown in detail in Figure 4b for Pd.

Two mechanisms were explored, oxidative addition followed by reductive elimination (Figure 4a) and insertion, followed by a β-OAc elimination pathway,[45] leading to Markovnikov and anti-Markovnikov products, and as anticipated, the former occurs with a lower energy requirement and is shown in Figure 4b for Pd. All higher energy mechanisms are described in detail in Supporting Information (Supporting Information, Figures S15−S17). The manifolds shown for palladium in Figure 4 are similar to those for nickel (Supporting Information, Figures S10−S14) and platinum (Supporting Information, Figures S18−S21), although they indicate a possibly different outcome for platinum compared with nickel and palladium.

For all three metals, insertion followed by a β-OAc-elimination pathway is favored over oxidative addition followed

Table 1. Rate Constants (k_{expt}) and Efficiencies (φ) for the Reaction of $[(phen)M(CH_3)]^+$ with Allyl Acetate

reactants	products	eq no.	k_{expt}[a]	φ[c] (%)
$[(phen)Ni(CH_3)]^+ + CH_3CO_2C_3H_5$	$[(phen)Ni(O_2CCH_3)]^+ + C_4H_8$	14	9.51×10^{-10}	36
	$[(phen)Ni(CH_3)(CH_3CO_2C_3H_5)]^+$	17	3.03×10^{-10}	11
	$[(phen)Ni(CH_3CO_2C_3H_4)]^+ + CH_4$	23	*b*	
$[(phen)Pd(CH_3)]^+ + CH_3CO_2C_3H_5$	$[(phen)Pd(O_2CCH_3)]^+ + C_4H_8$	14	7.11×10^{-10}	28
	$[(phen)Pd(CH_3)(CH_3CO_2C_3H_5)]^+$	17	5.41×10^{-10}	21
	$[(phen)Pd(CH_3CO_2C_3H_4)]^+ + CH_4$	23	*b*	
$[(phen)Pt(CH_3)]^+ + CH_3CO_2C_3H_5$	$[(phen)Pt(O_2CCH_3)]^+ + C_4H_8$	14	3.88×10^{-11}	2
	$[(phen)Pt(CH_3)(CH_3CO_2C_3H_5)]^+$	17	6.06×10^{-10}	24
	$[(phen)Pt(CH_3CO_2C_3H_4)]^+ + CH_4$	23	2.32×10^{-10}	10

[a]The collision rate was calculated using the theory of Su and Bowers[40] using the program COLRATE.[41] Errors are conservatively estimated as ±25%. The numbers listed represent the average of 3 runs. [b]Modeling suggests that the rate is negligible. [c]Reaction efficiency (φ) = $k_{expt}/k_{ADO} \times 100$.

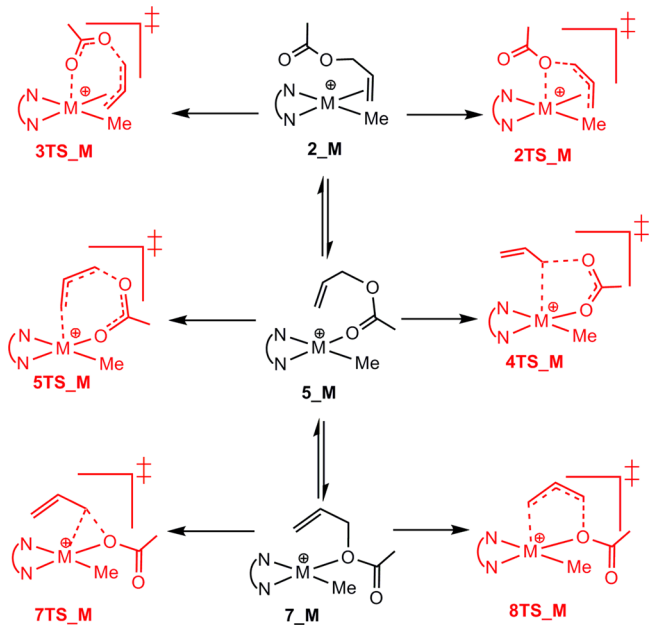

Figure 3. Overview of the six mechanisms explored for oxidative addition of allyl acetate to $[(phen)M(CH_3)]^+$ (M = Ni, Pd, Pt). For all three metals, the lowest energy process is via transition structure **4TS_M**, noting that **2_M** is the lowest energy structure for the three potential precursors shown here.

dx.doi.org/10.1021/jo501886w | J. Org. Chem. 2014, 79, 12056−12069

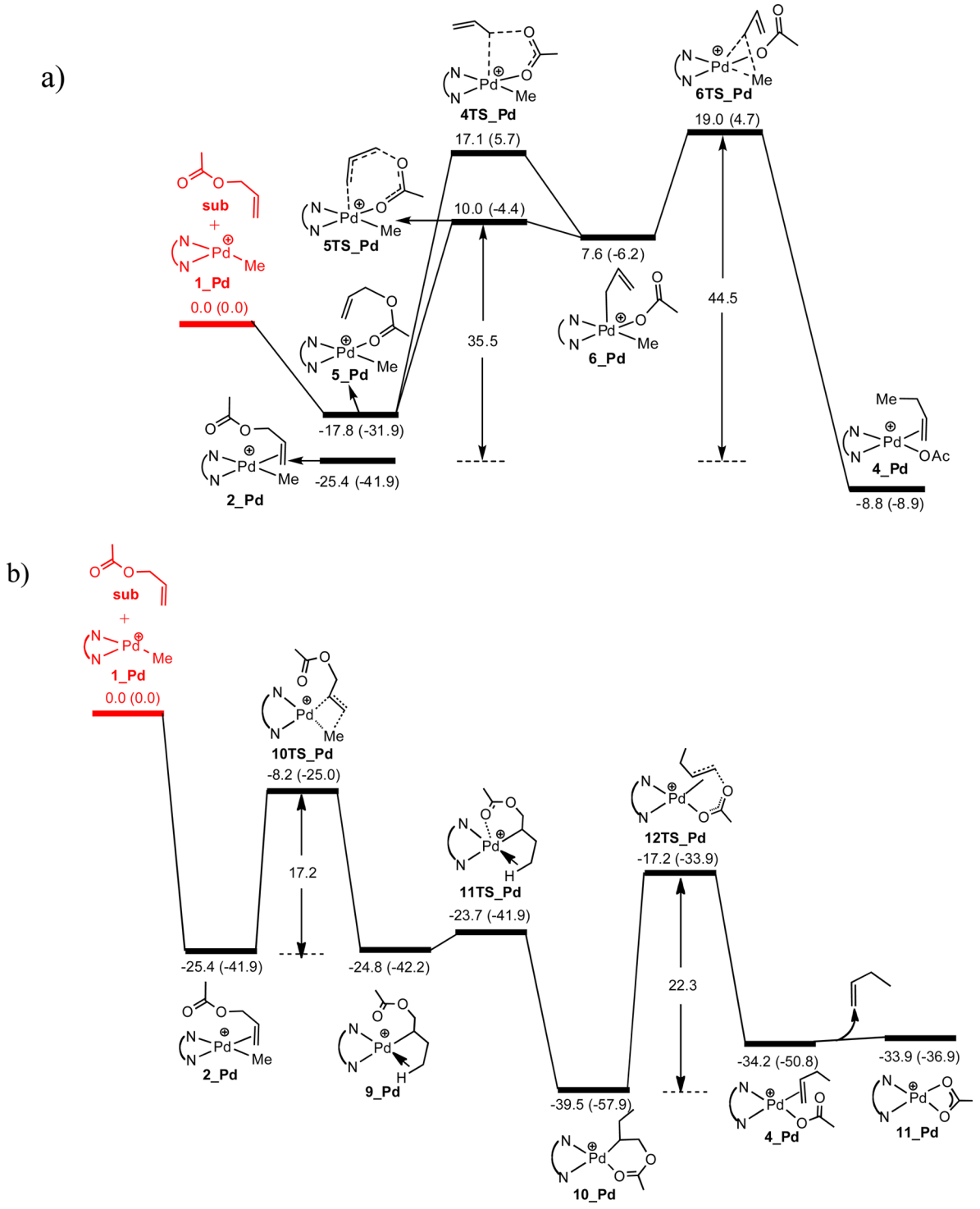

Figure 4. Results of DFT calculations at the M06/SDD6-31+G(d) level of theory. Plot of the potential energy diagram for the reaction of the complex $[(phen)Pd(CH_3)]^+$ with allyl acetate via (a) oxidative addition followed by reductive elimination or (b) an insertion reaction. Energies ΔG (ΔE) are given in kcal mol^{-1}.

by reductive elimination (Table S2 and Supporting Information, Figures S10−S21).

In addition to the lowest energy potential oxidative pathway, the structure of the simple allyl acetate complex (**2-Pd**) is also shown in Figure 4a in view of its role in the more favorable insertion process (Figure 4b).[46] In the oxidative process, addition of allyl acetate to $[(phen)Pd(CH_3)]^+$ (**1_Pd**) gives the O-coordinated $[(phen)Pd(CH_3)(CH_3CO_2C_3H_5)]^+$ (**5_Pd**), endergonically favored (ΔG −17.8 kcal mol^{-1}). However, the energy of subsequent key transition states is above that of the separated reactants for both oxidative addition pathways shown here, in particular **5TS_Pd** to form the Pd^{IV} complex **6_Pd**, and reductive elimination from this via **6TS_Pd**. Accordingly, the reaction is not expected to occur via this mechanism under the near thermal conditions of the ion trap;[47] thus although the details of this oxidative mechanism and others were explored

dx.doi.org/10.1021/jo501886w | J. Org. Chem. 2014, 79, 12056−12069

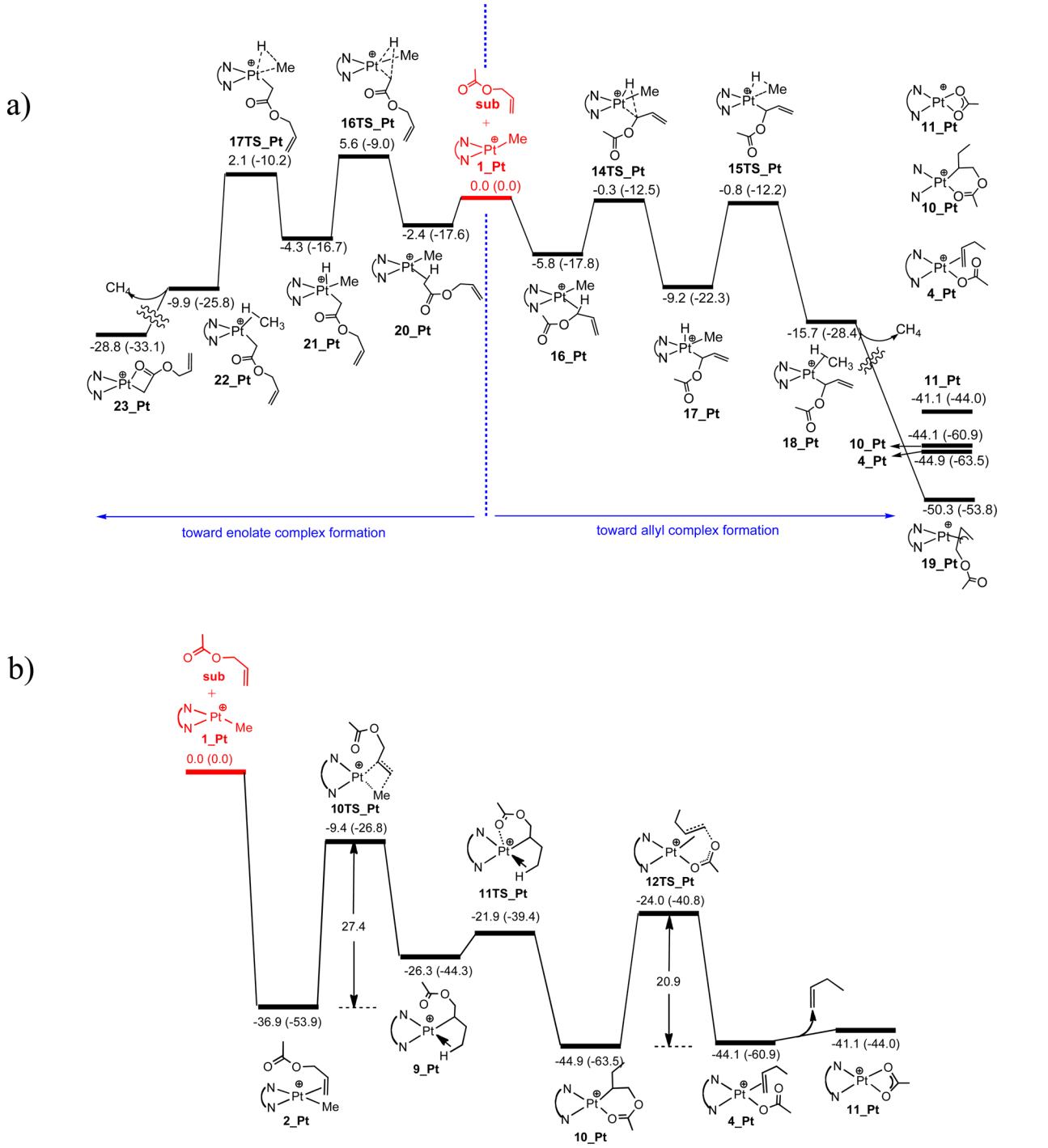

Figure 5. Results of DFT calculations at the M06/SDD6-31+G(d) level of theory. Plot of the potential energy diagram for the reaction of the complex $[(phen)Pt(CH_3)]^+$ with allyl acetate via (a) loss of CH_4 involving enolate formation (left) or allyl complex formation (right) or (b) C−C bond coupling via the insertion reaction. Energies ΔG (ΔE) are given in kcal mol^{-1}.

(Supporting Information, Figures S15−S17, S22), they are not discussed in detail.

In contrast, in Figure 4b the addition of allyl acetate as a conventional η^2-alkene donor in $[(phen)Pd(CH_3)]^+$ (**1_Pd**) is more favorable (25.4 vs 17.8 kcal mol^{-1} below the energy of the separated reactants).[48] All subsequent steps are also below the energy of the reactants. Insertion proceeds via transition structure **10TS_Pd**, conforming to the normal structure expected for insertion to give **9_Pd** containing an agostic interaction. A facile isomerization process then occurs via **11TS_Pd** to give **10_Pd**, which is finally followed by β-OAc elimination via **12TS_Pd**.[45] This insertion mechanism is similar to that proposed by Sawamura for the reaction of $[(phen)Pd(Ar)]^+$ with allyl acetates[18] and is the most likely pathway for the carbon−carbon bond formation reaction (eq 7). This same mechanism is also predicted to occur for the reaction of allyl acetate with $[(phen)Ni(CH_3)]^+$ (−8.0 kcal mol^{-1}) and $[(phen)Pt(CH_3)]^+$ (−8.2 kcal mol^{-1}).

The Case of Pt: Competing Mechanisms for CH_4 Loss and Relationship to C−C Bond Coupling. Two different general

dx.doi.org/10.1021/jo501886w | J. Org. Chem. 2014, 79, 12056−12069

Table 2. Summary of Decarboxylativeallylation Reactions of Allylacetate for Different Organometallic Catalysts

	decarboxylation (step 1)		allylic alkylation (step 2)	
catalyst	experimental yield (%)	DFT calculated activation energy (kcal mol^{-1})	experimental reaction efficiency (%) for C−C bond coupling	mechanism from DFT calculations
$[CH_3CuCH_3]^-$	>99[a]	38.5[a]	0.032[b]	OA/RE[b]
$[CH_3Cu_2]^+$	83.3[c]	46.4[c]	52.7[c]	OA/RE[c]
$[CH_3CuAg]^+$	20.4[c]	42.7[c]	1.2[c]	OA/RE[c]
$[CH_3Ag_2]^+$	44.5[c]	47.5[c]	0[c]	OA/RE[c]
$[(phen)Ni(CH_3)]^+$	87[d]	45.0[d]	47[e]	insert./β-OAc elim.[f]
$[(phen)Pd(CH_3)]^+$	95[d]	42.9[d]	49[e]	insert./β-OAc elim.[f]
$[(phen)Pt(CH_3)]^+$	100[d]	42.7[d]	2[f]	insert./β-OAc elim.[f]

[a]From ref 25a. [b]From ref 26e. [c]From ref 26f. [d]From ref 28. [e]This work. The efficiency of adduct formation and C−C bond formation are added together since CID on the adducts yields the C−C bond formation product. [f]This work.

mechanisms were examined for C−H activation of allyl acetate via addition with loss of CH_4 (eq 19): formation of the enolate, **23_Pt** (Figure 5a, left),[35] or the allyl complex, **19_Pt** (Figure 5a, right).[36,49] Both mechanisms proceed via insertion into a C−H bond to give the Pt(IV) complexes **21_Pt** (Figure 5a, left) and **17_Pt** (Figure 5a, right). Both reactions are exothermic overall. The enolate pathway has a slight kinetic barrier (**16_TS** and **17_TS**, 5.6 and 2.1 kcal mol^{-1} respectively). The deuterium labeling experiments, however, showed that the loss of methane can occur with loss of a hydrogen from the allyl group from the adduct to give $[(phen)Pt(CH_2CHCHO_2CCD_3)]^+$ (Supporting Information, Figures S2 and S3) or from the acetyl group to give $[(phen)Pt(CH_2CO_2CD_2CHCH_2)]^+$ (Supporting Information, Figures S4 and S5). These experimental results highlight that the deuterium isotope affects the bond energies and thus directs CH_4 loss from the nonlabeled site. Related CH_4 loss via C−H activation is a high energy process for Ni and Pd (Supporting Information, Figure S22), consistent with the fact that these reactions are not observed in the ion−molecule experiments (Figure 1a,b and Supporting Information, Figures S1−S3).

Inspection of Figure 5a,b, respectively, indicates that for the two competing pathways, **1_Pt** to **19_Pt** and **1_Pt** to **11_Pt**, the former can be regarded as the thermodynamic pathway and the latter as the kinetic pathway. Thus, although the initial intermediate **16_Pt** in Figure 5a is at substantially higher energy than the initial adduct **2_Pt** in Figure 5b, it leads to the thermodynamically preferred product **19_Pt**. All species formed in Figure 5b are lower in energy than **1_Pt**, and thus under the mass spectrometry conditions, the species preferred kinetically are able to equilibrate leading to **19_Pt**.

Comparisons with Previously Reported Decarboxylative Allylation Reactions of Allyl Acetate Catalyzed by Organometallic Ions in the Gas Phase. We have now described the decarboxylative allylation reactions of allyl acetate catalyzed by three different classes of organometallic ions: (1) the dimethyl cuprate anion, $[CH_3CuCH_3]^-$;[26e] (2) the clusters $[CH_3M1M2]^+$ (M1 = M2 = any combination of Ag and Cu);[26f] (3) the group 10 organometallic complexes, $[(phen)M(CH_3)]^+$ (this work). Table 2 summarizes these C−C coupling reactions.

$[CH_3CuCH_3]^-$ is formed in high yield via CID, consistent with it having the lowest decarboxylation barrier.[25a] It reacts with allyl acetate via several competing channels[26e] including C−C cross-coupling reactions, which is the most favored channel (Table 2, 81% yield), generating the product ion $[CH_3CO_2CuCH_3]^-$, and thus completing a catalytic cycle. However, the rate of the reaction was slow (11×10^{-13} cm^3·molecules^{-1}·s^{-1}) with reaction efficiency of only 0.032%. The lowest energy path found from DFT calculations involves stepwise π-oxidative addition proceeding via an η^2-$(C_3H_5O_2CCH_3)$ intermediate with extrusion of the acetate leaving group, followed by a reductive elimination where the acetate is recomplexed to the copper center.[26e]

All of the bimetallic systems $[CH_3M1M2]^+$ are formed upon decarboxylation, although the yield of $[CH_3Cu_2]^+$ is highest (83.3%). The allylic alkylation reactions of the bimetallic systems $[CH_3M1M2]^+$ with allyl acetate strongly depend on the nature of the metal. When one or both of the metals (M1 and M2) were silver, the C−C cross-coupling reaction channel either was very weak (1.2% yield, M1 = Cu and M2 = Ag) or did not proceed at all (M1 = Ag and M2 = Ag). The dicopper system ($[CH_3Cu_2]^+$)[26f] appears to have a good efficiency, good selectivity for the C−C cross-coupling reaction and the ability to complete a catalytic cycle. DFT calculations suggest that the most likely mechanism of this reaction involves discrete oxidative addition and reductive elimination steps, with both metal centers playing a role in both steps.[26f]

All of the group 10 organometallic cations $[(phen)M(CH_3)]^+$ are formed upon decarboxylation, and all undergo C−C bond coupling to close a catalytic cycle. In contrast to $[CH_3CuCH_3]^-$ and $[CH_3M1M2]^+$, these reactions proceed via insertion followed by β-OAc elimination, which is similar to that proposed by Sawamura (Scheme 2a).[18] Of all the catalysts studied thus far, the organometallic cations $[CH_3Cu_2]^+$ and $[(phen)Pd(CH_3)]^+$ are the best catalysts for both steps of the catalytic cycle. $[(phen)Ni(CH_3)]^+$ is also a promising catalyst.

CONCLUSIONS

A decarboxylative allylic alkylation carbon−carbon bond forming catalytic cycle using group 10 metal carboxylates in the gas phase has been demonstrated. The first step of the reaction occurs through decarboxylation of $[(phen)M(O_2CCH_3)]^+$ to form $[(phen)M(CH_3)]^+$, similar to a previously described protodecarboxylation reaction.[26] Mass spectrometry experiments, kinetic modeling, and DFT calculations were used to gain insights into the second step of this catalytic cycle, which involves C−C bond formation (eq 7). Experiments identified three types of products formed in the reactions of $[(phen)M(CH_3)]^+$ allyl acetate: (i) reformation of the carboxylate, $[(phen)M(O_2CCH_3)]^+$, completing the carbon−carbon bond formation catalytic cycle, which is the favored reaction for nickel and palladium; (ii) addition of allyl acetate to form an adduct $[(phen)M(C_6H_{11}O_2)]^+$; (iii) addition with concomitant loss of methane to form the ion $[(phen)M(C_5H_7O_2)]^+$ for platinum. Rate measurements show that the organometallic complex most favored to undergo carbon−

dx.doi.org/10.1021/jo501886w | J. Org. Chem. 2014, 79, 12056−12069

carbon bond formation upon addition of allyl acetate is $[(phen)Ni(CH_3)]^+$ followed by $[(phen)Pd(CH_3)]^+$ and then $[(phen)Pt(CH_3)]^+$.

Density functional theory calculations were used to examine two possible types of mechanisms for C−C bond formation: (a) oxidative addition, followed by reductive elimination, which involves changes in the oxidation state of the metal center; (b) an insertion reaction, which does not involve changes to the oxidation state of the metal center. For all metals, insertion mechanisms are predicted to be the most likely pathway for the C−C bond coupling reaction. It is of interest to consider the implications for solution phase chemistry of this mass spectrometric study of gas phase reactions. Similar conclusions can be drawn for nickel and palladium, in particular the oxidative process requires energies to reach transition structures that would be regarded as too high for all three metals (Ni, 33.8; Pd, 35.5; Pt 40.7 kcal mol^{-1}), linked to the positive charge on the reagent species. For platinum, DFT indicates kinetically (Figure 5b) and thermodynamically preferred pathways (Figure 5a) in competition for which, under mass spectrometry conditions, equilibration allows the thermodynamic pathway to be favored resulting in loss of methane and formation of an η^3-allyl platinum(II) product (Figure 5a). In solution, the thermodynamic pathway is considered to be inaccessible because the low energy adduct **2_Pt** initially formed by the reactants (Figure 5b) would require 36.9 kcal mol^{-1} to reform the isolated reactants to enter the process resulting in the thermodynamically preferred products. (Figure 5a).

Finally these gas-phase results coupled with a consideration of the previously reported cross coupling reactions shown in Scheme 2 suggest that the following new decarboxylative coupling reactions should be explored in solution: (i) $[(phen)Pd(O_2CAr)]^+$ with $ArCO_2Allyl$; (ii) $[(phen)Ni(O_2CAr)]^+$ with $ArCO_2Allyl$.

EXPERIMENTAL SECTION

Materials. $Pd(OAc)_2$, $Ni(OAc)_2$, K_2PtCl_4, and 1,10-phenanthroline were obtained from a chemical supplier (reagent grade). All solvents were HPLC grade. All purchased materials were used without further purification. $[(phen)Ni(O_2CCH_3)_2]$,[50] $[(phen)Pd(O_2CCH_3)_2]$,[51] and $[(phen)Pt(O_2CCH_3)_2]$[52] were prepared via literature methods and were characterized by exact mass measurements and examination of the isotopic pattern of the metal from high resolution mass spectrometry experiments on the mono acetate cations, $[(phen)M(O_2CCH_3)]^+$, formed via electrospray ionization in the positive ion mode (ion assignments available in Supporting Information, Table S1).

D3 allyl acetate, $CD_3CO_2CH_2CH{=}CH_2$, was prepared by an iron catalyzed reaction of allyl alcohol with D6 acetic anhydride using a modified literature procedure.[53] Briefly, $FePO_4$ (0.0075g, 0.05 mmol) was added to a mixture of allyl alcohol (0.058 g, 1.0 mmol) and deuterated acetic anhydride (0.270g, 2.5 mmol). The mixture was stirred overnight at room temperature with the product identified by TLC. CH_2Cl_2 (15 mL) was added, and the catalyst was filtered off. The product was neutralized by 15 mL of sodium bicarbonate (10%) and extracted with CH_2Cl_2. The organic phase was then dried using Na_2SO_4 and evaporated to give the product $CD_3CO_2CH_2CH{=}CH_2$. ^1H NMR: ($CDCl_3$, 600 MHz, TMS) δ 5.89 (dd, 1H), 5.30 (d, 1H), 5.21 (d, 1H), 4.54 (d, 2H).

Allyl-1-D2 acetate, $CH_3CO_2CD_2CH{=}CH$, was prepared using an adapted literature procedure.[53b] A mixture of anthracene (4.10 g, 23.0 mmol), methyl acrylate (5.90 g, 68.5 mmol, 6.22 mL), and xylene (100 mL) was stirred under reflux for 50 h. Solvent was removed *in vacuo*, and crystallization from pentane at 0 °C led to a light yellow solid (2.15 g, 8.07 mmol). The solid (5.07 g, 19.0 mmol) was dissolved in diethyl ether (150 mL), added slowly to a refluxing suspension of $LiAlD_4$ (1.20 g, 28.5 mmol) in diethyl ether (150 mL), and stirred at 80 °C for 16 h. The reaction was quenched with water and HCl solution (10%, 50 mL). The metal salt was filtered off, the organic layer was washed with saturated $NaHCO_3$ solution (2 × 40 mL) and dried with $MgSO_4$, and solvent was removed *in-vacuo* to give a pale yellow solid (4.55 g, 18.9 mmol). The solid (2.65 g, 11.0 mmol) was dissolved in dichloromethane (60 mL), and pyridine (1.40 g, 17.7 mmol, 1.43 mL) was added. Acetyl chloride (1.06 g, 13.5 mmol, 1.00 mL) in dichloromethane (25 mL) was slowly added at 0 °C, and the mixture was stirred at room temperature for 12 h. The reaction was quenched with water. The organic layer was washed with water (40 mL), HCl solution (10%, 40 mL), and saturated $NaHCO_3$ solution (40 mL) and dried with $MgSO_4$. Solvent was removed *in vacuo* to give a white solid (2.87 g, 10.2 mmol). The solid was heated with a bunsen burner under a vigreux column and an atmosphere of nitrogen gas. The product, which distilled off, was collected in a liquid nitrogen trap. Distillation of the product resulted in clear liquid $CH_3CO_2CD_2CH{=}CH$ (0.458 g, 4.48 mmol). ^1H NMR: ($CDCl_3$, 600 MHz, TMS) δ 5.90 (dd, J = 17.1, 10.5 Hz, 1H), 5.31 (d, J = 17.2 Hz, 1H), 5.23 (d, J = 10.4 Hz, 1H), 2.07 (s, 3H).

Mass Spectrometry Experiments. Mass spectrometric experiments were conducted on a Thermo Scientific (Bremen, Germany) LTQ FT hybrid mass spectrometer consisting of a linear ion trap (LTQ) coupled to a Fourier-transform ion cyclotron resonance (FT-ICR) mass spectrometer modified to allow ion−molecule reaction studies to be undertaken.[54] A recent study has demonstrated that under ion−molecule reaction conditions, collisions with the helium bath gas quasi-thermalizes the ions to room tempearture.[47]

The metal acetate complex cations, $[(phen)M(O_2CCH_3)]^+$, were formed via direct electrospray ionization of solutions of the acetates $[(phen)M(O_2CCH_3)_2]$ in water (~0.5 mM). The solution was introduced into the ESI source of the mass spectrometer at a flow rate of 5 μL/min. ESI conditions used were as follows: spray voltage 4.0 kV; capillary temperature 300 °C; nitrogen sheath gas flow rate ca. 10 arbitrary units. The three coordinate organometallic cations, $[(phen)M(CH_3)]^+$, were "synthesized" in the gas phase in a MS^2 experiment via low-energy collision induced dissociation (CID) of the mass selected metal carboxylate complex cations, $[(phen)M(O_2CCH_3)]^+$ in the linear ion trap. The helium bath gas was used as the collision gas at atmospheric pressure, and the CID conditions used included the following: a Q value of 0.25; an excitation time of 30 ms, with the normalized collisional energy varied from 0.3 to 1.1 V. Ion−molecule reactions between the mass selected organometallic cations, $[(phen)M(CH_3)]^+$, and allyl acetate were carried out in a series of MS^3 experiments with reaction times varying between 1 and 1000 ms. Single isotopes were selected (^{58}Ni, ^{106}Pd, and ^{195}Pt) to allow for distinction between complexes with similar mass to charge ratios such as $[(phen)^{60}Ni(CH_3)]^+$ and $[(phen)^{58}Ni(OH)]^+$.

Kinetic Modeling. The kinetics for the reaction between the organometallic ions of the form $[(phen)M(CH_3)]^+$ and allylacetate were examined using the LTQ FT hybrid mass spectrometer. Ion−molecule reaction rate measurements were conducted by isolating the reactant ion, $[(phen)M(CH_3)]^+$, in a MS^3 experiment and then allowing it to react with allylacetate, similar to previously reported ion−molecule reactions.[28,34] Single isotope peaks were used and three independent measurements were taken over 3 days. The mass selection windows and scan mass range were kept constant throughout. Theoretical rates for the reaction were calculated with the program COLRATE[41] using the average dipole orientation (ADO) theory of Su and Bowers.[40]

Theoretical Methods. Geometry optimizations and electronic energy calculations were performed using the Gaussian 09 molecular modeling package[55] to provide insights into the reactions of the organometallic cations, $[(phen)M(CH_3)]^+$, with allyl acetate. Structures of minima and transition states were optimized using the M06 hybrid functional.[56] The M06 functional was used because it reproduces properties in the Transition Metal Energetics (TME53) database to within 5.5 kcal mol^{-1}, on average (~0.24 eV),[57] to allow comparisons to previous work on the reactions of $[(phen)M(CH_3)]^+$ with water[34b] and acetic acid.[28] The Stuttgart Dresden (SDD) basis set

dx.doi.org/10.1021/jo501886w | J. Org. Chem. 2014, 79, 12056−12069

and effective core potential were used for the nickel, palladium, and platinum atoms, while the 6-31+G(d) all electron basis set was used for carbon, nitrogen, oxygen, and hydrogen. All optimized structures were subjected to vibrational frequency analysis to ensure they corresponded to true minima (no imaginary frequencies) or transition states (one imaginary frequency). IRC calculations were performed on transition states to confirm that minima and transition states correspond to the same potential energy surface.

■ ASSOCIATED CONTENT

Supporting Information

Cartesian coordinates of all species examined, a full citation of ref 55, ion−molecule reactions of $[(phen)M(CD_3)]^+$ with allyl acetate and $[(phen)M(CH_3)]^+$ and $[(phen)M(CD_3)]^+$ with $CD_3CO_2CH_2CH{=}CH_2$, ion−molecule reaction of $[(phen)Ni(OH)]^+$ with allyl acetate, ion−molecule reaction of $[(phen)M]^{+\bullet}$ (M = Ni and Pd) with allyl acetate and CID of the complexes $[(phen)M((CH_3CO_2C_3H_5]^{+\bullet}$, ion−molecule reaction of $[(phen)Pt(N_2)]^+$ with allyl acetate and table of high resolution mass spectra confirming ion assignments, and calculated potential energy diagram for the reaction of $[(phen)M(CH_3)]^+$ and allyl acetate proceeding via the oxidative addition/reductive elimination pathways and Markovinikov and anti-Markovinikov insertion pathways. This material is available free of charge via the Internet at This material is available free of charge via the Internet at http://pubs.acs.org.

■ AUTHOR INFORMATION

Corresponding Authors

*Phone: +613 6226 1744. Fax: +613 6226 2858. E-mail: Alireza.Ariafard@utas.edu.au.

*Phone: +613 8344-2452. Fax: +613 9347-5180. E-mail: rohair@unimelb.edu.au.

Notes

The authors declare no competing financial interest.

■ ACKNOWLEDGMENTS

We thank Dr. Gabriel da Silva for discussions on the kinetic modelling and the ARC for financial support via Grants DP110103844 (to R.A.J.O. and G.N.K.) and DP1096134 (to G.N.K.) and through the ARC CoE program and Grant DP120101540 (A.J.C. and B.F.Y.). M.W. thanks the Faculty of Science for a Melbourne Research Scholarship. The authors gratefully acknowledge the generous allocation of computing time from the Victorian Partnership for Advanced Computing (VPAC) Facility, the University of Tasmania, and the National Computing Infrastructure.

■ REFERENCES

(1) Fox, M. A.; Whitesell, J. K. *Organic Chemistry*, 3rd ed.; Jones and Bartlett: Sunbury, MA, USA, 2004; p 720.

(2) Another key class of reaction, which is being actively explored, is C−H functionalization: (a) Shilov, A. E.; Shul'pin, G. B. *Chem. Rev.* **1997**, *97*, 2879. (b) Jia, C.; Kitamura, T.; Fujiwara, Y. *Acc. Chem. Res.* **2001**, *34*, 633. (c) Labinger, J. A.; Bercaw, J. E. *Nature* **2002**, *417*, 507. (d) Godula, K.; Sames, D. *Science* **2006**, *312*, 67. (e) Bergman, R. G. *Nature* **2007**, *446*, 391. (f) White, M. C. *Synlett* **2012**, *23*, 2746.

(3) *Metal-Catalyzed Cross-Coupling Reactions*, 2nd ed.; de Meijere, A., Diederich, F., Eds., Wiley: Weinheim, Germany, 2004.

(4) Anastas, P. T.; Warner, J. C. *Green Chemistry: Theory and Practice*; Oxford University Press: New York, 1998; p 30.

(5) For reviews on the use of metal catalyzed decarboxylation reactions in synthesis, see: (a) Gooßen, L. J.; Gooßen, K.; Rodriguez, N.; Blanchot, M.; Linder, C.; Zimmermann, B. *Pure Appl. Chem.* **2008**, *80*, 1725. (b) Gooßen, L. J.; Rodriguez, N.; Gooßen, K. *Angew. Chem., Int. Ed.* **2008**, *47*, 3100. (c) Goossen, L. J.; Collet, F.; Goossen, K. *Isr. J. Chem.* **2010**, *50*, 617. (d) Rodriguez, N.; Goossen, L. *J. Chem. Soc. Rev.* **2011**, *40*, 5030. (e) Shang, R.; Liu, L. *Sci. China: Chem.* **2011**, *54*, 1670. (f) Cornella, J.; Larrosa, I. *Synthesis* **2012**, 653. (g) Dzik, W. I.; Lange, P. P.; Goossen, L. J. *Chem. Sci.* **2012**, *3*, 2671. (i) Gooßen, L. J.; Gooßen, K. *Top. Organomet. Chem.* **2013**, *44*, 121.

(6) Weaver, J. D.; Recio, A.; Grenning, A. J.; Tunge, J. A. *Chem. Rev.* **2011**, *111*, 1846.

(7) Burger, E. C.; Tunge, J. A. *J. Am. Chem. Soc.* **2006**, *128*, 10002.

(8) Pd(0) and Ni(0) C−C bond coupling reactions of allyl acetates in which the allyl group is utilized but the CH_3 group of the acetate is "wasted" have been known for decades. Pd: (a) Trost, B. M. *Acc. Chem. Res.* **1980**, *13*, 385. Ni: (b) Catellani, M.; Chiusoli, G. P.; Salerno, G.; Dallatomasina, F. *J. Organomet. Chem.* **1978**, *146*, C19. (c) Bricout, H.; Carpentier, J.-F.; Mortreux, A. *Tetrahedron Lett.* **1996**, *37*, 6105. (d) Leadbeater, N. E. *J. Org. Chem.* **2001**, *66*, 7539.

(9) (a) Louw, R.; Kooyman, E. C. *Rec. Trav. Chim.* **1965**, *84*, 1511−1525. (b) Louw, R.; Kooyman, E. C. *Rec. Trav. Chim.* **1967**, *86*, 147−155 and references cited therein.

(10) Pesci, L. *Atti Accad. Naz. Lincei* **1901**, *10*, 362.

(11) For reviews on the use of decarboxylation to form organometallics that have been isolated and characterized, see: (a) Deacon, G. B. *Organomet. Chem. Rev., Sect. A* **1970**, *5*, 355. (b) Deacon, G. B.; Faulks, S. J.; Pain, G. N. *Adv. Organomet. Chem.* **1986**, *25*, 237.

(12) (a) Whitmore, F. C.; Culhane, P. J. *J. Am. Chem. Soc.* **1929**, *51*, 602. (b) Whitmore, F. C.; Carnahan, F. L. *J. Am. Chem. Soc.* **1929**, *51*, 856.

(13) (a) Kharasch, M. S. *J. Am. Chem. Soc.* **1921**, *43*, 2238. (b) Kharasch, M. S.; Staveley, F. W. *J. Am. Chem. Soc.* **1923**, *45*, 2961.

(14) Shepard, A. F.; Winslow, N. R.; Johnson, J. R. *J. Am. Chem. Soc.* **1930**, *52*, 2083.

(15) (a) Nilsson, M. *Acta Chem. Scand.* **1966**, *20*, 423. (b) Nilsson, M.; Ullenius, C. *Acta Chem. Scand.* **1968**, *22*, 1998. (c) Chodowska-Palicka, J.; Nilsson, M. *Acta Chem. Scand.* **1970**, *44*, 3353.

(16) (a) Myers, A. G.; Tanaka, D.; Mannion, M. R. *J. Am. Chem. Soc.* **2002**, *124*, 11250. (b) Tanaka, D.; Romeril, S. P.; Myers, A. G. *J. Am. Chem. Soc.* **2005**, *127*, 10323. (c) Tanaka, D.; Myers, A. G. *Org. Lett.* **2004**, *6*, 433.

(17) (a) Goossen, L. J. *Appl. Organomet. Chem.* **2004**, *18*, 602. (b) Goossen, L. J.; Koley, D.; Hermann, H.; Thiel, W. *Chem. Commun.* **2004**, 2141. (c) Goossen, L. J.; Koley, D.; Hermann, H. L.; Thiel, W. *J. Am. Chem. Soc.* **2005**, *127*, 11102.

(18) (a) Ohmiya, H.; Makida, Y.; Tanaka, T.; Sawamura, M. *J. Am. Chem. Soc.* **2008**, *130*, 17276. (b) Ohmiya, H.; Makida, Y.; Li, D.; Tanabe, M.; Sawamura, M. *J. Am. Chem. Soc.* **2010**, *132*, 879. (c) Li, D.; Tanaka, T.; Ohmiya, H.; Sawamura, M. *Org. Lett.* **2010**, *12*, 3344. (d) Makida, Y.; Ohmiya, H.; Sawamura, M. *Chem.—Asian J.* **2011**, *6*, 410.

(19) (a) Yeagley, A. A.; Chruma, J. J. *Org. Lett.* **2007**, *9*, 2879. (b) Fields, W. H.; Khan, A. K.; Sabat, M.; Chruma, J. J. *Org. Lett.* **2008**, *10*, 5131. (c) Yeagley, A. A.; Lowder, M. A.; Chruma, J. J. *Org. Lett.* **2009**, *11*, 4022.

(20) Li, Z.; Jiang, Y. Y.; Yeagley, A. A.; Bour, J. P.; Liu, L.; Chruma, J. J.; Fu, Y. *Chem.—Eur. J.* **2012**, *18*, 14527.

(21) This contrasts with the Tsuji decarboxylative allylation reaction, for which decarboxylation has been suggested to occur at the metal center, with the resultant Pd(II) species undergoing an inner sphere reductive elimination reaction: (a) Sherden, N. H.; Behenna, D. C.; Virgil, S. C.; Stoltz, B. M. *Angew. Chem., Int. Ed.* **2009**, *48*, 6840. (b) Keith, J. A.; Behenna, D. C.; Sherden, N.; Mohr, J. T.; Ma, S.; Marinescu, S. C.; Nielsen, R. J.; Oxgaard, J.; Stoltz, B. M.; Goddard, W. A., III *J. Am. Chem. Soc.* **2012**, *134*, 19050.

(22) O'Hair, R. A. J. *Chem. Commun.* **2006**, 1469.

(23) *Theoretical Aspects of Transition Metal Catalysis*; Frenkin, G., Ed.; Springer: Berlin, 2005.

(24) O'Hair, R. A. J. Gas Phase Ligand Fragmentation to Unmask Reactive Metallic Species. In *Reactive Intermediates. MS Investigations in*

Solution.; Santos, L. S., Ed.; Wiley-VCH: Weinheim, Germany, 2010; Chapter 6, pp 199−227. ISBN: 978-3-527-32351-7

(25) (a) Rijs, N.; Waters, T.; Khairallah, G. N.; O'Hair, R. A. J. *J. Am. Chem. Soc.* **2008**, *130*, 1069. (b) Rijs, N. J.; Yates, B. F.; O'Hair, R. A. J. *Chem.—Eur. J.* **2010**, *16*, 2674. (c) Leeming, M.; Khairallah, G. N.; Osburn, S.; Vikse, K. L.; O'Hair, R. A. J. *Aust. J. Chem.* **2014**, *67*, 701.

(26) (a) James, P. F.; O'Hair, R. A. J. *Org. Lett.* **2004**, *6*, 2761. (b) Rijs, N. J.; Yoshikai, N.; Nakamura, E.; O'Hair, R. A. J. *J. Org. Chem.* **2014**, *79*, 1320. (c) Khairallah, G. N.; Waters, T.; O'Hair, R. A. J. *Dalton Trans.* **2009**, 2832. (d) Rijs, N. J.; Yoshikai, N.; Nakamura, E.; O'Hair, R. A. J. *J. Am. Chem. Soc.* **2012**, *134*, 2569. (e) Rijs, N. J.; O'Hair, R. A. J. *Organometallics* **2012**, *31*, 8012. (f) Al Sharif, H.; Vikse, K. L.; Khairallah, G. N.; O'Hair, R. A. J. *Organometallics* **2013**, *32*, 5416.

(27) For reviews on the role of gas phase experiments in uncovering the fundamental steps associated with catalysis, see: (a) Waters, T.; O'Hair, R. A. J. In *Fundamentals of and Applications to Organic (and Organometallic) Compounds*; Nibbering, N. M. M., Ed.; The Encyclopedia of Mass Spectrometry; Elsevier: Oxford, 2005; Vol. *4*, pp 604−612. (b) Bohme, D. K.; Schwarz, H. *Angew. Chem., Int. Ed.* **2005**, *44*, 2336. (c) Schwarz, H. *Angew. Chem., Int. Ed.* **2011**, *50*, 10096. (d) Castleman, A. W., Jr. *Catal. Lett.* **2011**, *141*, 1243. (e) Lang, S. M.; Bernhardt. *Phys. Chem. Chem. Phys.* **2012**, *14*, 9255. (f) Schlangen, M.; Schwarz, H. *Catal. Lett.* **2012**, *142*, 1265. (g) O'Hair, R. A. J. Mass Spectrometry Based Studies of Gas Phase Metal Catalyzed Reactions. *Int. J. Mass Spectrom.* **2014**, DOI: 10.1016/j.ijms.2014.05.003.

(28) Woolley, M. J.; Khairallah, G. N.; da Silva, G.; Donnelly, P. S.; O'Hair, R. A. J. *Organometallics* **2014**, *33*, 5185.

(29) The acetoxyl radical formed in eq 8 is likely to decarboxylate to give CH_3. and CO_2. For lead references, see: (a) Lu, Z.; Continetti, R. E. *J. Phys. Chem. A* **2004**, *108*, 9962. (b) Fraind, A.; Turncliff, R.; Fox, T.; Sodano, J.; Ryzhkov, L. R. *J. Phys. Org. Chem.* **2011**, *24*, 809. (c) Zhou, Y. Z.; Li, S.; Li, Q. S.; Zhang, S. W. *J. Mol. Struct. THEOCHEM* **2008**, *854*, 40 and references cited therein.

(30) There is considerable recent interest in the organic chemistry of high valent Pd complexes. For lead reviews, see: (a) Muñiz, K. *Angew. Chem., Int. Ed.* **2009**, *48*, 9412. (b) Xu, L. M.; Li, B. J.; Yang, Z.; Shi, Z. J. *Chem. Soc. Rev.* **2010**, *39*, 712. (c) Sehnal, P.; Taylor, R. J. K.; Fairlamb, I. J. S. *Chem. Rev.* **2010**, *110*, 824. (d) Hickman, A. J.; Sanford, M. S. *Nature* **2012**, *484*, 177. For a review on the reactivity of palladium complexes in oxidation states from 0 to IV of relevance to organic chemistry, see: (e) Bonney, K. J.; Schoenebeck, F. *Chem. Soc. Rev.* **2014**, *43*, 6609.

(31) Canty, A. J. *Acc. Chem. Res.* **1992**, *25*, 83.

(32) While the term isohypsic is typically used to describe reactions of organic compounds in which there is no change in oxidation state at a carbon centre, Hendrickson, J. B. *J. Am. Chem. Soc.* **1971**, *93*, 6847 its use here highlights reaction pathways in which the formal oxidation state of the metal remains unchanged.

(33) The neutral products of ion−molecule reactions are not detected and cannot be characterized in our experiments since they have no charge and cannot be trapped in the ion trap mass spectrometer. For rare examples of the isolation and characterization of neutral products of gas-phase ion−molecule reactions using a specialized apparatus, see: (a) Smith, M. A.; Barkley, R. M.; Ellison, G. B. *J. Am. Chem. Soc.* **1980**, *102*, 6851. (b) Jones, M. E.; Kass, S. R.; Filley, J.; Barkeley, R. M.; Ellison, G. B. *J. Am. Chem. Soc.* **1985**, *107*, 109.

(34) (a) Woolley, M.; Khairallah, G. N.; Donnelly, P. S.; O'Hair, R. A. J. *Rapid Commun. Mass Spectrom.* **2011**, *25*, 2083. (b) Woolley, M. J.; Khairallah, G. N.; da Silva, G.; Donnelly, P. S.; Yates, B. F.; O'Hair, R. A. J. *Organometallics* **2013**, *32*, 6931.

(35) For a book on the structure and chemistry of metal enolates, see: (a) *The Chemistry of Metal Enolates*; Zabicky, J., Ed.; The Chemistry of Functional Groups; Wiley: Chichester, 2009; ISBN: 9780470061688. For the formation and structural characterization of Pt(II) enolates with nitrogen donor ligands, see: (b) Vicente, J.; Abad, J. A.; Chicote, M.-T.; Abrisqueta, M.-D.; Lorca, J.-A.; Ramírez de Arellano, M. C. *Organometallics* **1998**, *17*, 1564. (c) Sharma, M.; Ariafard, A.; Canty, A. J.; Yates, B. F.; Gardiner, M. G.; Jones, R. C. *Dalton Trans.* **2012**, *41*, 11820. For the formation and structural characterization of Pd(IV) enolates with nitrogen donor ligands, see: (d) Byers, P. K.; Canty, A. J.; Skelton, B. W.; Traill, P. R.; Watson, A. A.; White, A. H. *Organometallics* **1992**, *11*, 3085.

(36) Pd allyl complexes play key roles in allylic alkylation reactions. For key reviews, see: (a) Consiglio, G.; Waymouth, R. M. *Chem. Rev.* **1989**, *89*, 257. (b) Trost, B. M.; Van Vranken, D. L. *Chem. Rev.* **1996**, *96*, 395. (c) Trost, B. M.; Crawley, M. L. *Chem. Rev.* **2003**, *103*, 2921. (d) Engelin, C. J.; Fristrup, P. *Molecules* **2011**, *16*, 951.

(37) The structure of these ions could in principle be established via IR spectroscopy. Gas-phase IR multiple-photon dissociation (IRMPD) spectroscopy of mass selected organometallic ions has been used to determine their IR spectra, thereby facilitating structure assignment. For a review, see: MacAleese, L.; Maître, P. *Mass Spectrom. Rev.* **2007**, *26*, 583.

(38) For studies that have used CID to establish the nature of related adducts, see ref 26f and (a) Robinson, P. S. D.; Khairallah, G. N.; da Silva, G.; Lioe, H.; O'Hair, R. A. J. *Angew. Chem., Int. Ed.* **2012**, *51*, 3812. (b) Vikse, K.; Naka, T.; McIndoe, J. S.; Besora, M.; Maseras, F. *ChemCatChem.* **2013**, *5*, 3604−3609.

(39) Kuzmic, P. *Anal. Biochem.* **1996**, *237*, 260.

(40) Su, T.; Bowers, M. T. *Int. J. Mass Spectrom. Ion Phys.* **1973**, *12*, 347.

(41) Lim, K. F. *Quantum Chem. Program Exch.* **1994**, *14*, 1.

(42) We note that since the effects of mass discrimination of ions in the ion trap during ion−molecule reactions are poorly understood, the raw ion abundances were used. It appears that in this case, mass discrimination does not have a significant influence on the determined rates because the total ion abundances do not change with reaction time. See Supporting Information, Figure S23, for a plot of total ion count vs time for a representative example.

(43) For reviews on the use of DFT calculations to examine Pd catalyzed cross coupling reactions, see: (a) Xue, L.; Lin, Z. *Chem. Soc. Rev.* **2010**, *39*, 1692. (b) García-Melchor, M.; Braga, A. A. C.; Lledós, A.; Ujaque, G.; Maseras, F. *Acc. Chem. Res.* **2013**, *46*, 2626.

(44) Oxidative addition of allylacetate to M(0) complexes (M = Ni or Pd) gives rise to M(II) complexes with coordinated allyl and acetate ligands. Ni: (a) Yamamoto, T.; Ishizu, J.; Yamamoto, A. *J. Am. Chem. Soc.* **1981**, *103*, 6863. Pd: (b) Yamamoto, T.; Saito, O.; Yamamoto, A. *J. Am. Chem. Soc.* **1981**, *103*, 5600. (c) Yamamoto, T.; Akimoto, M.; Saito, O.; Yamamoto, A. *Organometallics* **1986**, *5*, 1559.

(45) For key literature on β-OAc elimination, see: (a) Zhao, H.; Ariafard, A.; Lin, Z. *Organometallics* **2006**, *25*, 812. (b) Le Bras, J.; Muzart, J. *Tetrahedron* **2012**, *68*, 10065.

(46) For DFT calculations on the competition between O-coordination and η^2-alkene coordination in the reaction of acrolein with $[(bpy)Pd(C_2H_3)]^+$, see: Peng, Q.; Yan, H.; Zhang, X.; Wu, Y.-D. *J. Org. Chem.* **2012**, *77*, 7487.

(47) Donald, W. A.; Khairallah, G. N.; O'Hair, R. A. J. *J. Am. Soc. Mass Spectrom.* **2013**, *24*, 811.

(48) Allyl carboxylates and related compounds form η^2-alkene complexes with Pt(II): (a) Briggs, J. R.; Crocker, C.; McDonald, W. S.; Shaw, B. L. J. *J. Organomet. Chem.* **1979**, *131*, 213. For related examples from DFT calculations on Pd(0) complexes, see: (b) Fristrup, P.; Ahlquist, M.; Tanner, D.; Norrby, P.-O. *J. Phys. Chem. A* **2008**, *112*, 12862.

(49) The activation of the allylic C−H bond adjacent to the acetate group in allyl acetate appears to be unprecedented. In contrast, there are examples of allylic C−H bond activation remote from acyl groups: (a) Chen, M. S.; White, M. C. *J. Am. Chem. Soc.* **2004**, *126*, 1346. (b) Chen, M. S.; Prabagaran, N.; Labenz, N. A.; White, M. C. *J. Am. Chem. Soc.* **2005**, *127*, 6970. (c) Qi, X.; Rice, G. T.; Lall, M. S.; Plummer, M. S.; White, M. C. *Tetrahedron* **2010**, *66*, 4816.

(50) Ye, B.-H.; Chen, X.-M.; Xue, G.-Q.; Ji, L.-N. *J. Chem. Soc., Dalton Trans.* **1998**, 2827.

(51) Milani, B.; Alessio, E.; Mestroni, G.; Sommazzi, A.; Garbassi, F.; Zangrando, E.; Bresciani-Pahor, N.; Randaccia, L. J. *Chem. Soc., Dalton Trans.* **1994**, 1903.
(52) (a) Price, J. H.; Williamson, A. N.; Schramm, R. F.; Wayland, B. B. *Inorg. Chem.* **1972**, *11*, 1280. (b) Fanizzi, F. P.; Natile, G.; Lanfranchi, M.; Tiripicchio, A.; Laschi, F.; Zanello, P. *Inorg. Chem.* **1996**, *35*, 3173. (c) Soro, B.; Stoccoro, S.; Minghetti, G.; Zucca, A.; Cinellu, M. A.; Gladiali, S.; Manassero, M.; Sansoni, M. *Organometallics* **2005**, *24*, 53.
(53) (a) Behbahani, F. K.; Farahani, M.; Oskooie, H. A. *J. Korean Chem. Soc.* **2011**, *55*, 633. (b) Bartlett, P. D.; Tate, F. A. *J. Am. Chem. Soc.* **1953**, *75*, 91.
(54) Donald, W. A.; McKenzie, C. J.; O'Hair, R. A. J. *Angew. Chem., Int. Ed.* **2011**, *50*, 8379.
(55) Frisch, M. J.; et al. *Gaussian 09*, revision A.02; Gaussian, Inc., Wallingford CT, 2009.
(56) (a) Zhao, Y.; Schultz, N. E.; Truhlar, D. G. *J. Chem. Theory Comput.* **2006**, *2*, 364. (b) Zhao, Y.; Truhlar, D. G. *J. Chem. Phys.* **2006**, *125*, No. 194101. (c) Zhao, Y.; Truhlar, D. G. *J. Phys. Chem. A* **2006**, *110*, 13126.
(57) Zhao, Y.; Truhlar, D. G. *Theor. Chem. Acc.* **2008**, *120*, 215.